

Pitfalls when simulating 40/100G upgrade of legacy 10G WDM transmission systems

Hadrien Louchet¹, André Richter
VPIsystems, Carnotstr. 6, 10587 Berlin, Germany

Abstract

We detail a methodology to avoid pitfalls while investigating the upgrade of legacy 10G transmission systems with 40G DP-BPSK or 100G DP-QPSK channels using numerical simulation. Techniques for efficient and accurate estimation of intra- and inter-channel nonlinear effects are discussed.

Keywords: Fiber optics communications, coherent, 100G, XPM, XpolM

1. Upgrade of legacy 10 & 40G systems

The increasing demand for bandwidth- and cost-effective 100G Ethernet interfaces has urged the need to upgrade legacy transmission systems with 100G channels. Replacing existing 10G channels by 100G ones first looks unproblematic as the 100G channels based on the standardized coherent DP-QPSK technology fit in the 100GHz and 50GHz frequency grids and present relaxed requirements with regards to linear transmission impairments like chromatic dispersion (CD) and polarization effects. However, the presence of channels with different baud-rates as well as the use of dual polarization (DP) intensifies the impact of cross-phase and cross-polarization modulation effects (XPM, XpolM). Both effects are of statistical nature as they depend on the bit-pattern and state of polarization (SOP) of neighboring channels as well as on the fiber birefringence profile. In addition, other effects like coherent cross-talk lead to statistical variations of the system performance and should be therefore carefully simulated. In this paper, efficient simulation methods to estimate accurately impairments induced by these effects are presented. Simulations are carried out using *VPItransmissionMaker 8.6*.

2. Single channel performance

First of all, the performance of newly added 40G or 100G channel must be investigated in single-channel configurations. In order to identify the optimal input power, the *achievable OSNR* and the OSNR required to achieve a target BER (usually 10^{-3}) should be plotted on the same graph versus the channel input power (see for instance Figure 2). The minimum value of the *required OSNR* (ROSNR) depends on the modulation format and baud-rate as well as on the transmitter and receiver design. Transmission impairments such as tight-filtering, XPM and XpolM result in an increase of the ROSNR nominal value whereas intra-channel nonlinear effects lead to an input-power dependent ROSNR for the considered channel (see Figure 2).

2.1 Tight filtering

Tight filtering, for instance induced by (reconfigurable) optical add-drop multiplexers, (R)OADM, can result in an increase of the ROSNR i.e. in a degradation of the system performance. For example, particular care should be taken when deploying 112Gb/s DP-QPSK (28Gbaud) or 45Gb/s DP-BPSK (22.5Gbaud) on a system with 50GHz frequency grid. The OSNR penalty due to cascaded 1st order optical Gaussian filters (emulating the wavelength selective switches in the OADM) with 50 or 60GHz 3dB bandwidth is displayed in Figure 1 (left) for 112Gb/s DP-QPSK.

2.2 Cross-talk

Linear impairments consisting of incoherent and coherent cross-talk taking place at the optical cross connects (OXC) lead to statistic variations of the system performance. For instance the ROSNR for a 112Gb/s DP-QPSK channel has been estimated in presence of cross-talk due to a (non-ideally) dropped 10Gb RZ channel. 50 different states of the 10G RZ channel (relative SOP and delay with regard to the 100G channel) have been considered for each cross-talk value. The results are reported in Figure 1 (right) and show important fluctuations of the ROSNR for realistic cross-talk values

¹ Hadrien.Louchet@VPIphotonics.com; phone +49 303980580; www.VPIphotonics.com

(-20 dB). Note that impairments are maximized when the SOP of the 10G channel is aligned with one of the DP-QPSK tributaries.

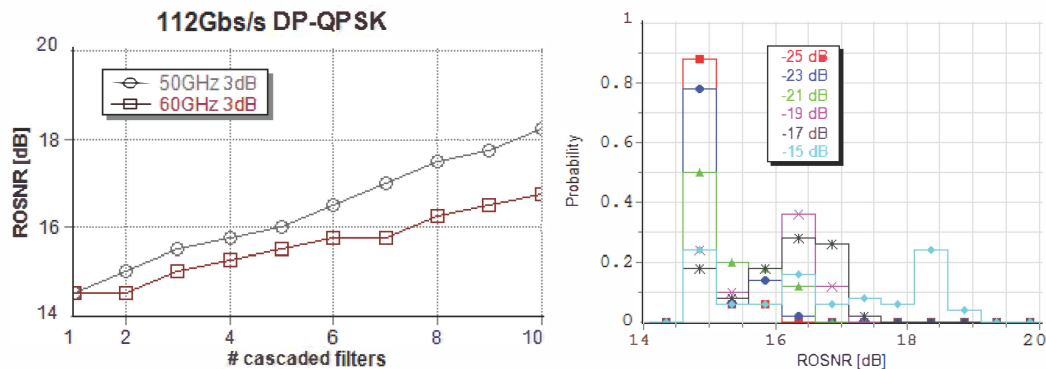


Figure 1: Left: ROSNR for a 112Gb/s DP-QPSK channel vs. number of cascaded optical filters. Right: channel performance for varying level of cross-talk in OXC.

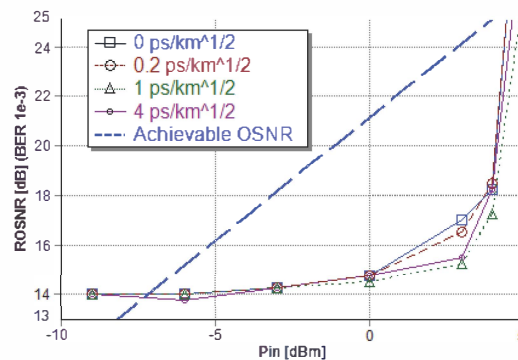


Figure 2: ROSNR vs. input power of 112G DP-QPSK in single channel configuration (20 x 80km G652 fiber, 1% residual dispersion per span for different PMD values).

2.3 Intra-channel effects

The required OSNR in presence of intra-channel effects can be estimated by simulating the channel propagation in an ASE-noise free transmission line for different input powers and by adding ASE-noise in front of the receiver. In absence of linear impairments (CD and PMD are compensated in front of the receiver), the required OSNR versus input power can be expressed as sum of the required OSNR in back-to-back configuration plus the OSNR penalty due to intra-channel nonlinearities. In real systems linear effects such as CD and PMD are mitigated using Digital Signal Processing (DSP) after coherent detection. Perfect compensation cannot be achieved, though, due to the limited speed and accuracy of the electronic circuits, and the performance of the implemented algorithms themselves, which cannot remove completely these effects when other impairments such as nonlinear effects or cross-talk occur simultaneously. In numerical simulations linear effects can be ideally removed by measuring the Jones matrix of the (linear) transmission line and applying its inverse in front of the receiver. It becomes possible to focus on the impact of nonlinearities only.

Since intra-channel effects such as iFWM and iXPM in a 100G DP-QPSK channel are only weakly PMD-dependent (see Figure 2), simulating the channel propagation over a single realization of the fiber's birefringence profile for each span is sufficient to characterize the system performance. Nonlinear propagation is simulated using either the Manakov-PMD equation or the coupled nonlinear Schrödinger equation. Both can be solved by combining the split-step and coarse-step methods and become equivalent for long fibers (>50 km) with random birefringence and non-zero PMD. As the targeted raw BER in modern transmission systems with FEC is around 10^{-3} , Monte-Carlo simulations can be used to obtain accurate estimates. To speed up the simulation, the propagation of a relatively short symbol sequence (hundreds of

symbols) can be simulated in an ASE-noise free system. This sequence is then duplicated N times in front of the receiver with a new realization of the optical noise added to each copy. Since intra-channel nonlinear effects are strongly pattern-dependent in dispersion-managed (DM) systems, we suggest using k-ary De Bruijn sequences for simulation. For example, a 4-ary De Bruijn sequence of order 7 ensures that all possible transitions between 7 successive QPSK symbols are present in the simulated signal sequence, and would therefore enable to account accurately for nonlinear inter-symbol interferences for 28Gbaud signals in SSMF-based DM systems.

3. WDM performance

3.1 XPM and XpolM

In DM systems using G652 fibers and 50GHz (or more) channel spacing, four wave mixing can be neglected and the main nonlinear impairments are due to XPM and XpolM. XpolM is an inter-channel effect resulting in fast polarization-modulation, and therefore depolarization of the transmitted signal, which manifests itself in fading and channel cross-talk for dual-polarization signals. Investigating any particular channel (*probe*) XpolM-induced depolarization depends on the variance of the Stokes vector of the aggregate co-propagating channels (*pumps*). Expressed in Stokes space, the variation of the probe signal SOP described by its Stokes vector \vec{s} is given by:

$$\frac{\partial \vec{s}}{\partial z} = \frac{8}{9} \gamma \vec{s}_T \times \vec{s} \quad (1)$$

\vec{s}_T being the Stokes vector of the aggregated probe and pump signals. Note that (1) can be written as $\vec{s}/\partial z \approx 8/9 \gamma \vec{p} \times \vec{s}$ when the power of the pump is much larger than the one of the probe signal, i.e. XpolM leads to a rotation of the probe channel Stokes vector around the one of the pump.

In order to illustrate the impact of XpolM, the probe SOP evolution over the transmission line is displayed in Figure 3 assuming CW pump and probe. For sake of simplicity, a loss- and dispersion-less fiber with constant birefringence has been considered so that the SOP of the probe and pump remain constant over the transmission line (in linear regime). The results are reported for different pump SOPs. When the launched SOPs of the probe and pump are identical (or orthogonal) no polarization modulation takes place.

The fact that the SOP of probe and pump evolve randomly over the transmission due to CD and PMD makes the XpolM effect pattern-dependent and stochastic. Therefore, the numerically predicated system performance may present large statistical variations depending on the simulated fiber birefringence [1] and on the relative SOP of the interacting channels [2]. These issues are discussed in the following sections.

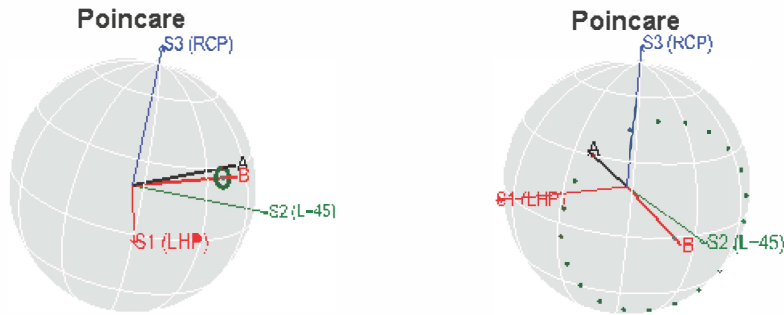


Figure 3: Evolution of the probe SOP along the transmission line (green circles) for different launch SOPs of probe (A) and pump (B).

3.2 Fiber birefringence profile

To illustrate the statistical nature of XPM and XpolM-induced impairments, we first consider the propagation of one 112Gb/s DP-QPSK channel surrounded by six 10Gb/s RZ channels on a 100GHz grid over a 20 spans system. Each span consists of 80km of G652 fiber, a DCF module and an EDFA. The EDFA is assumed noise-less, and the DP-QPSK input power is set to -6dBm in order to focus on XPM and XpolM effects only. The input power of the 10G channels is set to

4dBm. The ROSNR values for the 112Gb/s channels are gathered for 50 different fiber birefringence profiles assuming a PMD of 0.2 and 0.06 ps/sqrt(km) are displayed in Figure 4 (left: as an histogram, right: versus channel depolarization). The depolarization of the DP-QPSK channel is defined as $\langle |\Delta \hat{\mathbf{S}}| \rangle / |\hat{\mathbf{S}}|^2$ where $\hat{\mathbf{S}}$ is the original SOP of the channel and $\Delta \hat{\mathbf{S}}$ its variation measured in the middle of a DP-QPSK symbol at the receiver. Note that in this investigation, the starting SOP of the 10G channels have been assumed identical and aligned with the X tributary of the 112Gb/s DP-QPSK channel.

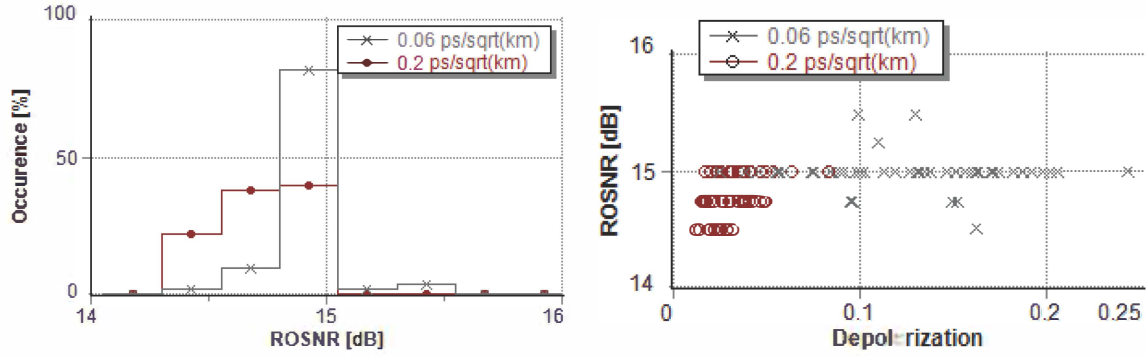


Figure 4: Performance of the 112Gb/s D-QPSK channel surrounded by six legacy 10G channels gathered over 50 different fiber birefringence profiles with 0.06 and 0.2 ps/sqrt(km) PMD.

3.3 Channels state of polarization

The best & worst cases regarding the relative SOP of the 100G and 10G channels have been discussed in [2]. The worst case has been shown to be the one maximizing XpolM, i.e. when the azimuth of the pump is rotated by 45° with respect to the SOP of the orthogonal tributaries of the DP-QPSK channel. On the contrary, aligning the SOP of the 10G channels with one of the tributaries will maximize the XPM-induced jitter in this polarization, and therefore result in different behaviors of the DP-QPSK tributaries [3].

Controlling the relative SOPs of the 100G and 10G channels is difficult as different lasers are used for the transmitters, and the channels' relative SOP does not remain constant along the line as a result of PMD. Below we report results of two sets of simulations. In the first one, we assumed an identical SOP for all six 10G channels. The required OSNR values are reported versus azimuth and ellipticity defined with respect to the SOP of the X tributary in Figure 5 (left), and versus signal depolarization in Figure 5 (right). The fibers PMD parameter has been set to 0.6 ps/sqrt(km).

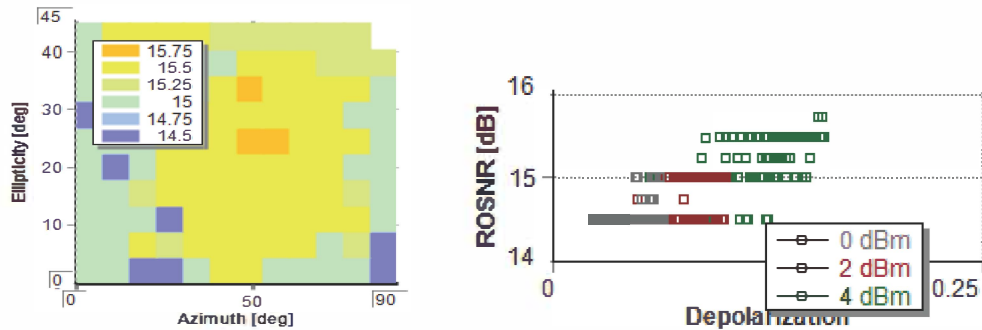


Figure 5: ROSNR for the 112Gb/s DP-QPSK channel versus SOP of the 10G channels (4dBm input power) (left), and depolarization (right).

In the second set of simulations, we assumed random starting SOPs for all six 10G channels resulting therefore in depolarized XPM-XpolM 'pumps'. 100 different starting SOP configurations have been simulated. The resulting ROSNR of the 112Gb/s DP-QPSK channel is reported as histogram and versus signal depolarization in Figure 6 for the case of aligned SOPs (left) and random SOPs (right) of the six 10G channels.

Results show that the system performance strongly depends on the SOP of the pump (*aggregate 10G channels*). However, no significant differences are observed in the performance statistics of systems with a polarized pump (Figure 6, left) and a depolarized pump (Figure 6, right). This is due to the fact that a polarized pump becomes quickly depolarized as a result of PMD.

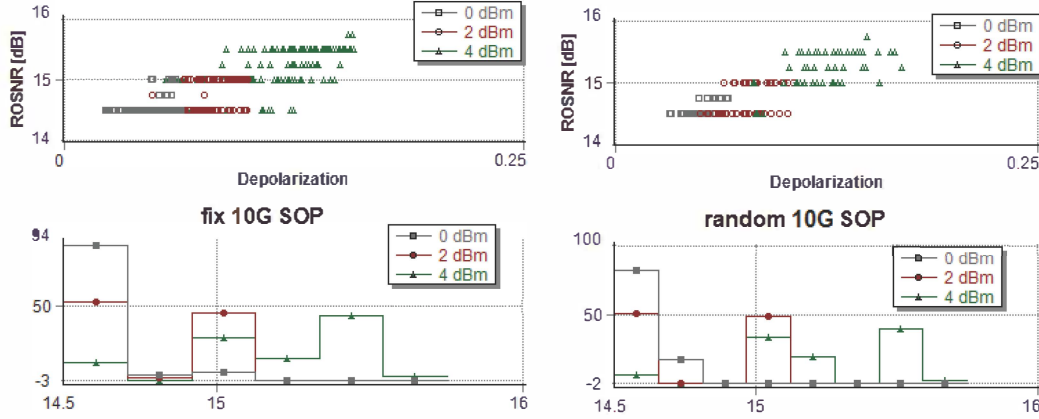


Figure 6: System performance with aligned (left) or random (right) SOP for the 10G channels.

3.4 PMD

We further investigate the impact of PMD, by considering a PMD value of 0, 0.1 and 0.2 ps/sqrt(km) for the fibers. As discussed in [3] and shown in Figure 4, large PMD values reduce the impact of XpolM, and therefore the statistical variation of the system performance resulting from fiber birefringence. This averaging effect also reduces the impact on the system performance of the relative starting SOP between the channels (see Figure 7). As a result, the number of simulation runs (different starting SOP, fiber birefringence profiles) required to characterize the system performance is significantly reduced in a system using old fibers presenting large PMD.

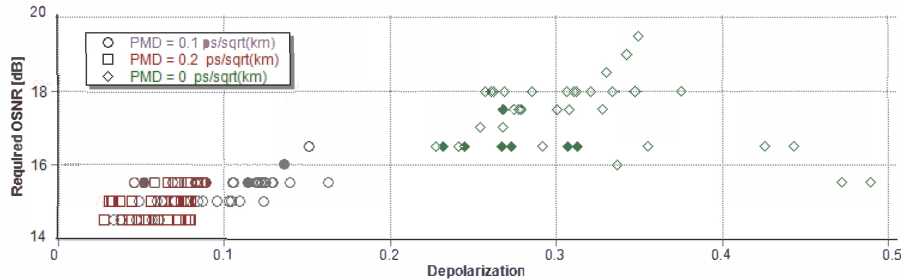


Figure 7: Required OSNR vs. depolarization for 50 different birefringence profiles of the transmission line (20 x 80km G652, 1% residual dispersion per span) with six 10G neighboring channels (3dBm input power) for different PMD values (from [2]).

3.5 Number of neighboring channels

The numerical results reported in [1], validate the analytical models reported in [4-5] which predict that signal distortions induced by inter-channel effects grow with the logarithm of the number of neighboring channels. This is an important result as it shows that even though the impact of channels located far away from the probe channel cannot be completely ignored, it can be extrapolated.

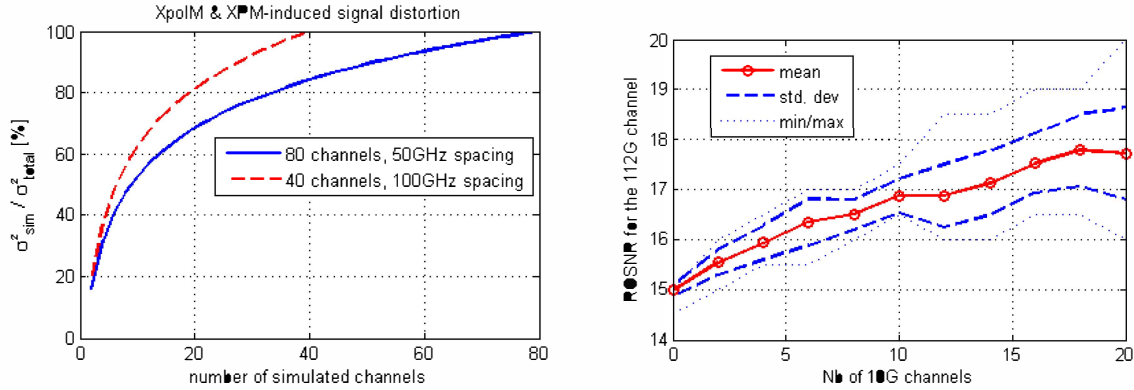


Figure 8: left: Mean magnitude of XPM and XpolM-induced distortions versus number of co-propagating 10G channels. Right: ROSNR [dB] of a 112G DP-QPSK channel vs. number of co-propagating 10G RZ channel.

The results reported in [1] show that a large number of channels need to be simulated to achieve an acceptable accuracy. This effort is much larger than what is usually suggested in the literature [6]. The dependency as predicted by [4] is illustrated in Figure 8, left for different WDM configurations (50 and 100GHz channel spacing). For the considered systems, simulating half of the channels will result in underestimating XPM and XpolM-induced distortions of 1dB. Note that simulating the whole C and/or L band is now feasible using commercial tools implementing graphics processing unit (GPU) – supported simulations.

To illustrate this point, the propagation of a 112Gb/s DP-QPSK signal has been numerically estimated for a 10 spans transmission line with G652 fibers (PMD=0.2 ps/sqrt(km)) with 1% residual dispersion per span in presence of a varying number of 10Gb/s RZ channels on a 100GHz grid. The starting SOP of the 10G channels have been assumed independent from each other and 20 different starting SOP realizations have been simulated. The input power of the 112 and 10G channels has been set to -6 and -3dBm respectively. The mean max and minimum ROSNR (1e-3 BER) for the 112Gb/s DP-QPSK signal is displayed in Figure 8 and confirm the analytical predictions.

4. Conclusions

We detailed a methodology to avoid pitfalls when simulating mixed bit rates systems including 10G legacy and 40G DP-BPSK or 100G DP-QPSK channels. A particular focus has been made on the accurate and efficient simulation of fiber nonlinearities. We showed that system performance can present significant fluctuations when XPM and XpolM effects are strong. Therefore we suggest simulating the investigated system using different fiber birefringence profiles as well as different configurations for the starting channels SOP in order to obtain an accurate statistical characterization of the system performance.

References

- [1] C. Xia et al., in *Proc OFC 2011*, OWO1.
- [2] D. Sperti et al., in *Proc. Fotonica 2010*, A2.4
- [3] H. Louchet et al., in *Proc. ICTON 2011*, We.B1.1
- [4] H. Louchet et al., *IEEE Photon. Technol. Lett.*, **15**, 1219-12-21 (2003)
- [5] P. Poggiolini et al., *IEEE Photon. Technol. Lett.*, **23**, 742-744 (2011)
- [6] M. Bertolini et al. *Opt. Fiber Technol.*, **16**, 274-278, (2010)